www.coast.osustech.edu.ng
COAST
JOURNAL OF THE FACULTY OF SCIENCE
Volume 1, Issue 2. March, 2020 ISSN: 2714-3716
Coast, J. Fac. Sci. 1 (2): 225 - 231

EFFECTS OF PRESSURE GRADIENT ON REACTIVE FLOW IN ROTATING CONCENTRIC CYLINDER

[1]Usman, M. A and [2*]Badejo, O. M

[1]Department of Mathematical Sciences, Olabisi Onabanjo University, Ago Iwoye, Ogun State, Nigeria.
[2*]Department of Mathematical Sciences, Ondo State University of Science and Technology, Okitipupa.
Corresponding author's e-mail: badeomi@yahoo.com

Abstract
Flow over rotating cylinders is very important in a wide number of applications from shafts and axles to spinning projectiles. This can sustain lives or put lives at serious risk which may lead to death sometimes. That is why this work investigates unsteady reactive flow of rotating concentric cylinder (annulus) with reactive term with both cylinders rotating in opposite direction. The cylinder's length is finite and the reactive proximity is fixed to be 0.50mm, considering the effect of pressure gradient (G) on magnetic field on other parameters. The governing equations on reactive flow in a rotating concentric cylinder were derived. Guided by related journal's results on reactive flow in a rotating concentric cylinder which are applicable to moving machine systems. The incompressible with constant density governing equation were used to investigate the impacts of magnetic force, pressure gradient, velocity, temperature and the flow rate of the fluids in the rotating concentric cylinder (annulus). The energy equations were formulated with reactive term for proper results justification. The unsteady and one-dimensional equations and axial symmetric flow of the Newtonian fluid in the rotating concentric cylinder with fixed proximity and boundary conditions were investigated. Finite difference method with MAPLE 2014 software, was used for the interpretation of figures and the results were in agreement with the reviewed journal.

Keywords: Reactive Term, Concentric Cylinder, Annulus, Magnetic Field and Pressure Gradient

Introduction

A fluid dynamics analysis of the velocity and pressure fields was studied in the annular gap between two concentric cylinders with a stationary outer cylinder and a rotating inner cylinder is presented. Both the transient and steady-state velocity and pressure profiles of an isothermal, Newtonian fluid are considered. The effect of varying the angular velocity of the inner cylinder, fluid viscosity and radius of the inner cylinder on the fluid velocity and pressure profiles are examined. The results show that the fluid velocity profiles approach a fully-developed state only after travelling a distance that is much greater than the annular gap between the cylinders. It is also shown that the pressure exerted on the inner cylinder increases monotonically with rotational speed. Results that illustrate the potential utility of using cross-platform finite element analysis, solver and multiphysics simulation software (COMSOL Multiphysics) to study the fluid flow stability and parametric behaviour are also illustrated (Barman, *et al* (2015).

The classical Couette flow problem consists of infinitely long concentric cylinders and an incompressible Newtonian fluid between them. For a system with a rotating inner cylinder and a stationary outer cylinder, the fluid flow passed on stable circular Couette flow and steady axisymmetric Taylor vortex flow for the value of Taylor number *Ta* (or Reynolds number Re) less than and greater than a critical value *Ta*c (or Rec*)* respectively (Shu *et al* 2004).

Mamunur (2008) studied a detailed computational investigation on the Newtonian fluid flow through concentric annuli with centre body rotation with glucose as the working fluid. A confined flow through concentric annuli with centre body rotation was examined numerically by solving the modified Navier-Stokes equations. He measured the axial and tangential components of velocity presented in non-dimensional form for a Newtonian fluid. The annular geometry consists of a rotating Centre body with angular speed of 126 rpm and a radius ratio of 0.506. He integrated continuity and the momentum equations numerically with the aid of a finite – volume method.

Ali (2002) estimated concentric annular flows of Newtonian fluids in vertical and horizontal arrangements based on computational fluid dynamics simulations, but did not quantify the effects of internal shaft rotation. A Mathematical model was presented for the steady, axisymmetric, magnetohydrodynamic (MHD) flow of a viscous, Newtonian, incompressible, electrically-conducting liquid in a highly porous regime intercalated between two concentric rotating cylinders in the presence of a radial magnetic field. The porous medium was modeled using a Darcy-Forchheimer drag force approach to simulate the impedance effects of the porous medium fibers at both low velocities and also at higher velocities, was studied by Beg *et al.*, (2012).

In a resent paper Aberkane *et al.* (2014) studied the effect of an axial magnetic field imposed on incompressible flow of electrically conductive fluid between two horizontal coaxial cylinders. The imposed magnetic field was assumed uniform and constant. The effect of heat generation due to viscous dissipation was also taken into consideration. The inner and outer cylinders are maintained at different uniform temperatures and concentrations. The movement of the fluid was due to the reaction of the cylinder with a constant speed. An exact solution of the governing equations for momentum and energy are obtained in the form of Bessel functions. A finite difference implicit scheme was used in the numerical solution to solve the governing equations of convection flow and mass transfer. The velocity, concentration and temperature distributions was obtained with and without the magnetic field.

El-Amin, (2003) shown that heat transfer and fluid flow over a non-isothermal horizontal cylinder in a porous medium can be controlled using electromagnetic fields. The Aim of this work is to determine effects of pressure gradient on reactive flow in rotating concentric cylinder by examining the steady flow in a concentric cylinder with and without reactive term considering magnetic field on pressure gradient, energy dissipation, porosity and suction parameter.

Mathematical Formulations

This section considered a system with reactive term flow in between concentric cylinders rotating simultaneously, unsteady state, laminar, and fully developed flow of fluids for which the density and the viscosity are constant.

The governing Navier-Stoke equations are:

Continuity equation

$$\frac{\partial}{\partial r}(ur) = 0 \qquad (1)$$

Momentum equation

$$\frac{\partial u}{\partial t} = v\left[\frac{\partial^2 u}{\partial r^2} + \frac{\partial}{\partial r}\left(\frac{u}{r}\right)\right] - \frac{1}{\rho}\frac{\partial P}{\partial r} - \frac{\sigma u B_0{}^2}{\rho} - \frac{vu}{K} - \frac{\Gamma u^2}{K} \qquad (2)$$

Energy equation

$$\frac{\partial T}{\partial t} = \frac{u}{r}\frac{\partial}{\partial r}\left(r\frac{\partial T}{\partial r}\right)K + \mu\left(\frac{\partial u}{\partial r} - \frac{u}{r}\right)^2 + QC_0Ae^{\left(\frac{E}{RT}\right)} \qquad (3)$$

Therefore, u is the velocity, V is the fluid kinematic viscosity, r is the radius, $\frac{u}{r}$ is the rotating parameter in the governing partial differential equations.

Equations (3) is the energy equations with reactive term. The last term in equation (3) is the reactive term.

The Boundary Conditions are:

$$r = r_1, \quad u = r_1\omega, \qquad r = r_2, \quad u = r_2\omega \qquad (4)$$

Dimensionless Form

Dimensionless Parameters

$$U = \frac{u}{\omega b}, R = \frac{r}{b}, T = \frac{t}{t_0}, \theta = \frac{T}{T_0}, V_0 = \frac{\omega}{b}, V = \frac{\mu}{\rho} \qquad (5)$$

These can also be written in these forms

$$u = U\omega b \qquad r = Rb \qquad t = Tt_0$$
$$T = \theta T_0 \qquad \omega = \quad V_0 b \qquad \mu = V\rho \qquad (6)$$

Substituting equation (6) into equations (2) yields

$$\frac{\partial U}{\partial T} = \frac{\partial^2 U}{\partial R^2} + \frac{1}{Re}\frac{\partial}{\partial R}\left(\frac{U}{R}\right) + \frac{G}{Re} - \frac{Ha^2}{Re}U - \frac{1}{Da}U - \frac{Fs\,Re}{Da}U^2 \qquad (7)$$

Substituting equation (6) into equations (3) yields

$$\frac{\partial \theta}{\partial T} = \frac{V_0}{Pr}\left(\frac{U}{R}\right)\frac{\partial}{\partial R}\left(R\frac{\partial \theta}{\partial R}\right) + Ec\left[\left(\frac{\partial U}{\partial R}\right)^2 - 2\frac{U}{R}\left(\frac{\partial U}{\partial R}\right) + \left(\frac{U}{R}\right)^2\right] + \gamma e^{\left(\frac{1}{\varepsilon}\right)} \qquad (8)$$

Where:

$$Re = \frac{\omega_2 b^2}{v}v \ ; \ Fs = \frac{\Gamma}{b} \ ; \ Da = \frac{r}{b^2} \ ; \ Ha^2 = \frac{\sigma B_0^2 b^2}{\mu} \ ; \ \gamma = \frac{QC_0 t_0}{T_0 b^2}$$
$$Pr = \frac{b^2}{Kt_0} \ ; \ Ec = \frac{\mu\omega_2^2 t_0}{T_0 b^2} \ ; \ V_0 = \frac{\omega_2}{b} \ ; \ G = -\frac{\partial P}{\partial R}; \ \varepsilon = \frac{RT_0}{E}$$

Definition of Symbols

B_0: Magnetic Field, **σ**: Fluid Electrical Conductivity, ***v***: Fluid Kinematic Viscosity

K: Porus Medium Permeability, **Γ**: Forchheimer Geometric Inertial drag parameter

V_0: Suction Parameter, ρ: Fluid Density, G Pressure Gradient, Q: Heat Reaction

A: Rate Constant, *E*: Activation Energy, *R* Universal Gas Constant

C_0**:**Initial Concentrating of the Reacting Species, γ:Frank-Kamenetskii Parameter

Re: Reynolds Number, **Ha:** Hartmann Number, **Da:** Darcy Number, **Pr:** **P**randtl Number **Ec:** Eckert Number

The Boundary Conditions also yield

$$R = \frac{r_1}{b} \qquad U = \frac{r_1\omega}{\omega_2 b} \qquad (9)$$

Results and Discussion

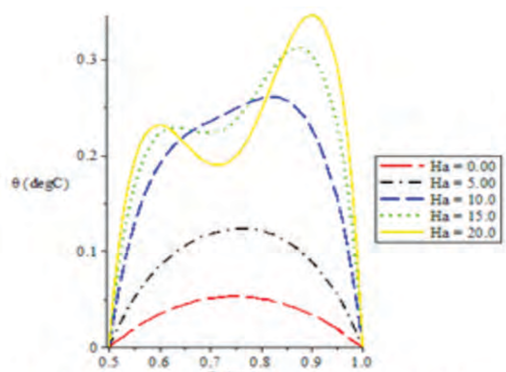

Fig 1A The Temperature profile θ (deg C) versus Cylindrical radius R (mm) for values of Hartmann number (Ha) with reactive term, when $Ec = 1$, R = 1, $Da = 1$, $G = 0$, $Fs = 0.5$, $V_0 = 1$ & $Pr = 1$

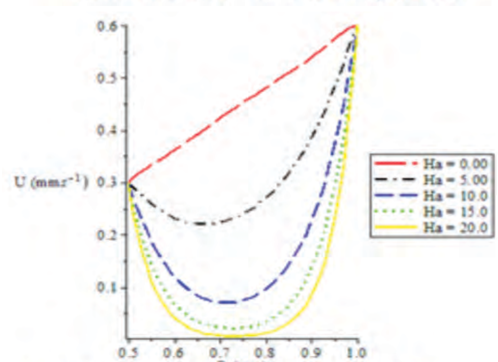

Fig 1B The Velocity profile U(mm s-1) versus Cylindrical radius R (mm) for values of Hartmann number (Ha) when R = 1, $Da = 1$, $G = 0$, $Fs = 0.5$ & $V_0 = 1$.

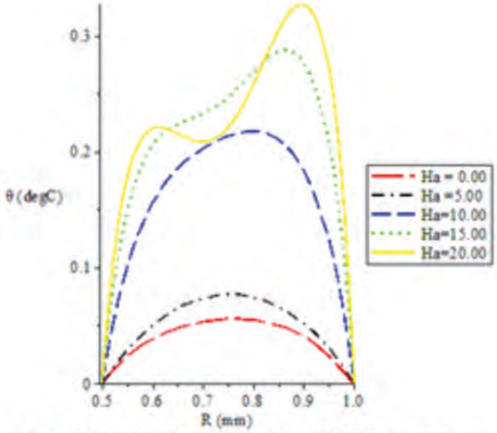

Fig 2A The Temperature profile θ (deg C) versus Cylindrical radius R (mm) for values of Hartmann number (Ha) with reactive term, when $Ec = 1$, $R = 1$, $Da = 1$, $G = 5$, $Fs = 0.5$, $V_0 = 1$ & $Pr = 1$

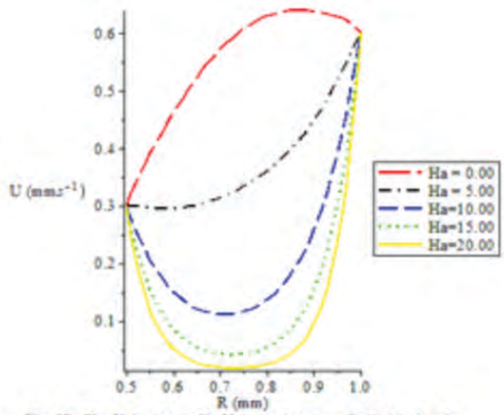

Fig 2B The Velocity profile U (mms-1) versus Cylindrical radius R (mm) for values of Hartmann number (Ha) with reactive term, when $R = 1$, $Da = 1$, $G = 5$, $Fs = 0.5$ & $V_0 = 1$.

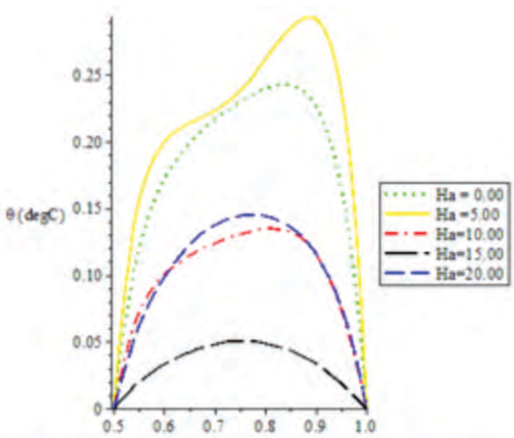

Fig 3A The Temperature profile θ (deg C) versus Cylindrical radius R (mm) for values of Hartmann number (Ha) with reactive term, when $Ec = 1$, $R = 1$, $Da = 1$, $G = 15$, $Fs = 0.5$, $V_0 = 1$ & $Pr = 1$

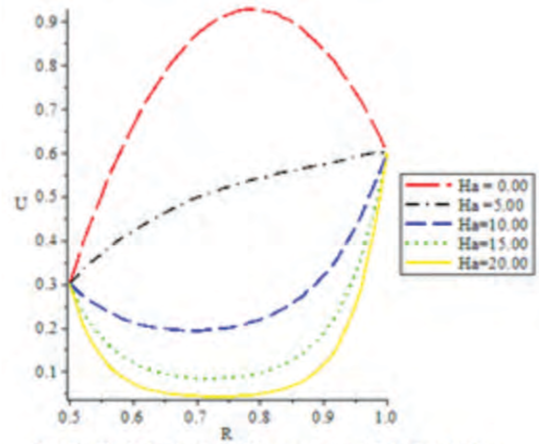

Fig 3B The Velocity profile U(mms-1) versus Cylindrical radius R (mm) for values of Hartmann number (Ha) when $R = 1$, $Da = 1$, $G = 15$, $Fs = 0.5$ & $V_0 = 1$.

Fig. 1A, Fig. 2A and Fig. 3A present the Temperature profiles versus Universal gas constant for various values of Hartmann number (Ha) with reactive term. The temperature of the system seems to be increasing and stable when the pressure gradient is zero (0) or not visible as Hartmann number varies from 0 to 10 and become stable as the Hartmann number is more than 10. Also the temperature of the system reduced as the pressure gradient increased.

Fig. 1B, Fig. 2B and Fig. 3B show the velocity profile for values of Hartmann number (Ha) from 0.00 to 20.00 when the pressure gradient is 0, 5 and 15 respectively and as the Hartmann number increases the velocity of the system reduces. Considering a case of no pressure gradient when Hartmann number is also at rest the graph is straight. Also, when the pressure gradient is 5 the highest velocity is 0.60 while the highest velocity of Fig. 3A is 0.90 then the Hartmann number (Ha) at zero becomes curve but in opposite direction to other values of Hartmann number. The higher the pressure gradient the more the velocity values of the system.

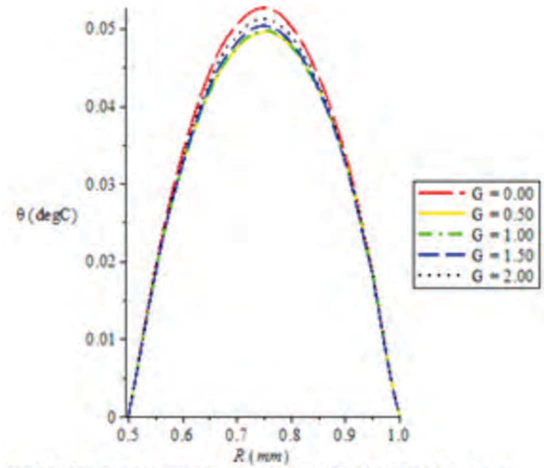

Fig.4A The Temperature profile θ (deg C)) Cylindrical radius R (mm) for values of Pressure Gradient (G) with reactive term, when $Ec = 1$, $R = 1$, $Da = 1$, $Ha = 0$, $Fs = 0.5$, $V_0 = 1$ & $Pr = 1$

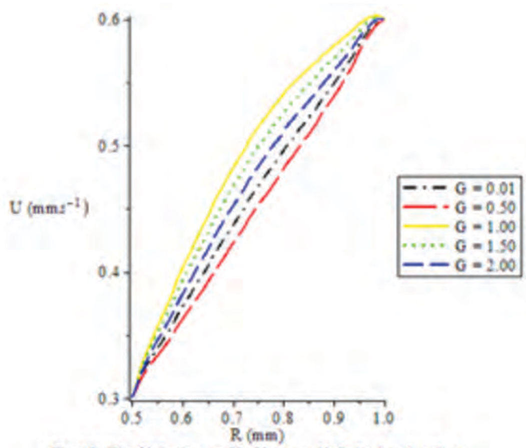

Fig.4B The Velocity profile U (mms-1) Cylindrical radius R (mm) for values of Pressure Gradient (G) when $R = 1$, $Da = 1$, $Ha = 0$, $Fs = 0.5$ & $V_0 = 1$.

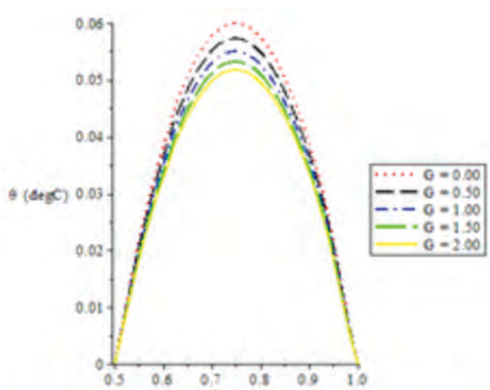

Fig. 5A The Temperature profile θ (deg C) versus Cylindrical radius R (mm) for values of Pressure Gradient (G) with reactive term, when $Ec = 1$, $R = 1$, $Da = 1$, $Ha = 2$, $Fs = 0.5$, $V_0 = 1$ & $Pr = 1$

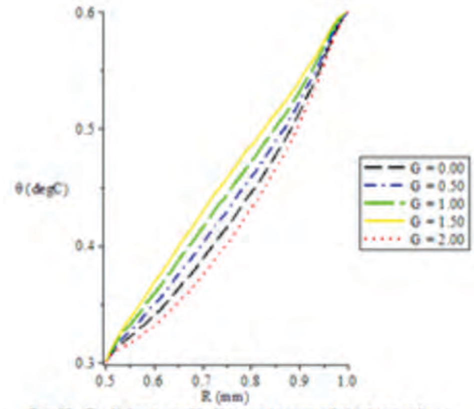

Fig. 5B The Velocity profile U (mms-1) versus Cylindrical radius R (mm) for values of Pressure Gradient (G) when $\Re = 1$, $Da = 1$, $Ha = 2$, $Fs = 0.5$ & $V_0 = 1$.

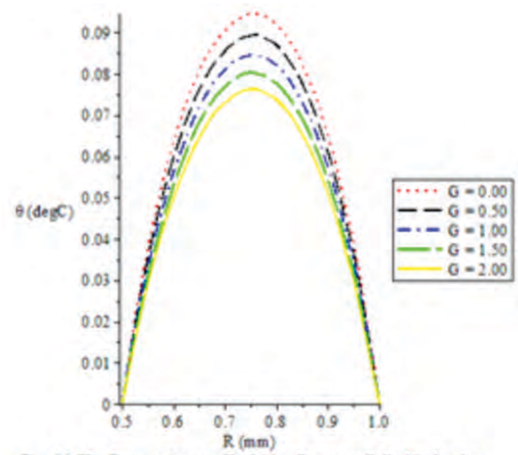

Fig. 6A The Temperature profile θ (deg C) versus Cylindrical radius R (mm) for values of Pressure Gradient (G) with reactive term, when $Ec = 1$, $R = 1$, $Da = 1$, $Ha = 4$, $Fs = 0.5$, $V_0 = 1$ & $Pr = 1$

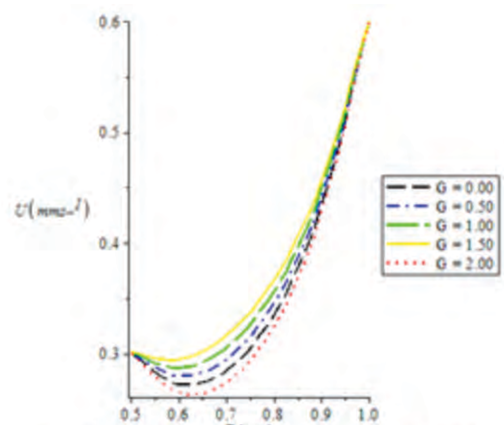

Fig. 6B The Velocity profile U (mms-1) versus Cylindrical radius R (mm) for values of Pressure Gradient (G) when $R = 1$, $Da = 1$, $Ha = 4$, $Fs = 0.5$ & $V_0 = 1$.

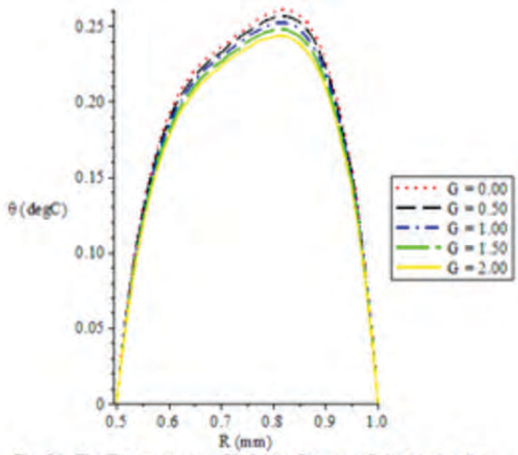

Fig 7A The Temperature profile θ (deg C) versus Cylindrical radius R (mm) for values of Pressure Gradient (G) with reactive term, when $Ec = 1$, $R = 1$, $Da = 1$, $Ha = 10$, $Fs = 0.5$, $V_0 = 1$ & $Pr = 1$

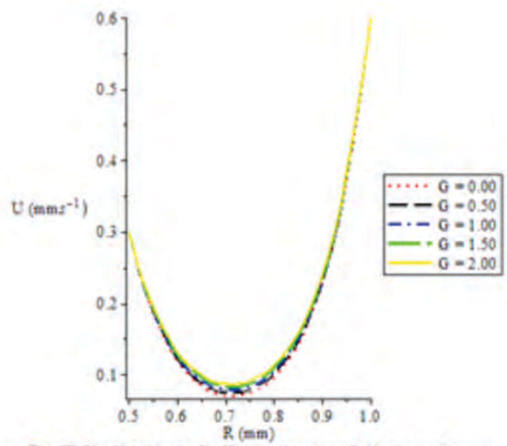

Fig 7B The Velocity profile U (mms-1) versus Cylindrical radius R (mm) for values of Pressure Gradient (G) when $R = 1$, $Da = 1$, $Ha = 10$, $Fs = 0.5$ & $V_0 = 1$.

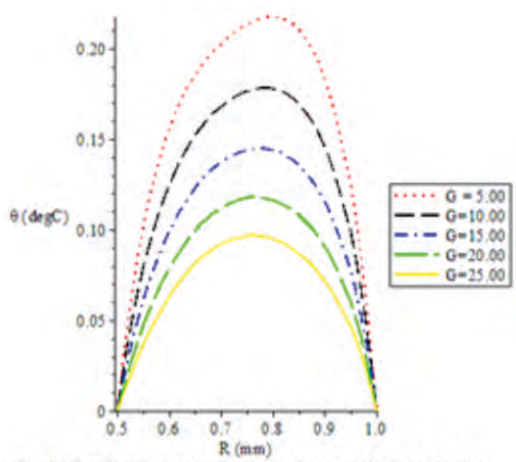

Fig 8A The Temperature profile θ (deg C) versus Cylindrical radius R (mm) for values of Pressure Gradient (G) =5 to 25 with reactive term, when $Ec = 1$, $R = 1$, $Da = 1$, $Ha = 10$, $Fs = 0.5$, $V_0 = 1$ & $Pr = 1$

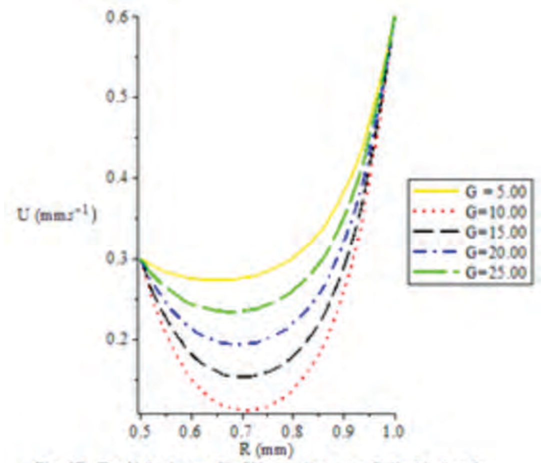

Fig 8B The Velocity profile U(mms-1) versus Cylindrical radius R(mm) for values of Pressure Gradient (G) = 5 to 25 when $R = 1$, $Da = 1$, $Ha = 10$, $Fs = 0.5$ & $V_0 = 1$.

Fig. 4B, Fig. 5B, Fig. 6B, Fig. 7B and Fig. 8B also show the velocity profile of Hartmann number (Ha=0.2,4,10) on the pressure gradient (G) and it was observed that as the pressure gradient (G) increases the velocity decreases and this made the system to be stable. Also as the Hartmann number increases from 3.00 to 5.00 it brings the velocity deflection closer.

Fig. 4A, Fig. 5A, Fig. 6A, Fig. 7A and Fig. 8A show the temperature profile for values of hartmann number from zero (0) to 10 on pressure gradient with reactive term. This figure is not that stable when the value of Hartmann number (Ha) is zero (0) on pressure gradient. The highest temperature is above 0.05 as the pressure gradient increases the temperature reduces. When the Hartmann number (Ha) increases from 2 to 10 the temperature is stable and highest temperature of Fig. 5A, Fig. 6A, Fig. 7A and Fig. 8A are 0.06, 0.09, 0.26 and 0.25 respectively. It was also observed that as the pressure gradient (G) increased the temperature reduced.

Conclusion

It was observed that the pressure gradient reduces the temperature of a system, as the pressure gradient increases the temperature reduces. Hartmann number (Ha) increases the temperature without the effect of pressure gradient.

Reference

Aberkane S., Malika I., Moderres M. and Abderrahmane G (2014). Effect of axial magnetic field on the heat and mass transfer in rotating annulus, *Inter J Physical Sci*, 9(16): 368-379.

Ali A. W. (2014). The Effect of the Inner Cylinder Rotation on the Fluid Dynamics of Non-newtonian. *Brazilian J Chemical Engrn*, 31(4): http://dx.doi.org/10.1590/0104-6632.20140314s00002871

Barman K., Mothupally S., Sonejee A., and Mills P. L, (2015). Fluid Motion Between Rotating Concentric Cylinders Using COMSOL Multiphysics, *Oral presentation given at the COMSOL 2015 Conference,* Boston, session on Computational Fluid Dynamics.

Beg O. A., Makinde O. D., Swapan J. Z. and Ghosh S. K., (2012). Hydro magnetic viscous flow in a rotating annular high-porosity medium with nonlinear forcheimer drag effects: numerical study, *World J Modelling and Simulation*. 8(2); 83-95.

El-Amin, M.F (2003). Combined effect of viscous dissipation and joule heating on MHD forced convection over a non-isothermal horizontal cylinder embedded in a fluid saturated porous medium, *J Magnetism and Magnetic Materials*, 263; 337–343.

Mamunur R (2008). CFD for Newtonian Glucose fluid flow through concentric annuli with centre body rotation, *Inter J Sci Techn (IJSAT)*, 2(5);180 – 186.

Shu C., Wang L., Chew Y. T and Zhao N., (2004). Numerical Study of Eccentric Couette – Taylor Flows and Effect of Eccentricity on Flow Patterns. *Theoretical Computational Fluid Dynamics*, 18. 43 – 59.